Proc. 17th Int. Symp. on Mathematical Theory of Networks and Systems, 2006

Leadership in Animal Group Motion: A Bifurcation Analysis

Benjamin Nabet, Naomi E. Leonard, Iain D. Couzin and Simon A. Levin

***Abstract*— We present a low-dimensional, continuous model of a multi-agent system motivated by simulation studies on dynamics of decision making in animal groups in motion. Each individual moves at constant speed in the plane and adjusts its heading in response to relative headings of others in the population. Two subgroups of the population are informed such that individuals in each subgroup have a preferred direction of motion. The model exhibits stable solutions corresponding to compromise by individuals with conflicting preferences. We study the global phase space for the proposed model by computing equilibria and proving stability and bifurcations.**

***Keywords*— Coordinated motion, Bifurcation analysis.**

I. INTRODUCTION

In this paper we study the dynamics of a low-dimensional, minimally parameterized, cooperative control system, motivated by an interest in modelling and predicting the behavior of animal groups in motion. Many social organisms move in groups when they forage or migrate, and it is thought that the movement decisions they make may depend on social interactions among group members [1], [2], [3].

In Couzin et al [3], the mechanisms of decision-making and leadership are investigated using a discrete simulation of particles moving in the plane. In this simulation, each particle represents an individual animal and the motion of each individual is influenced by the state of its neighbors (e.g., relative position and relative heading). Within this group, there are two subgroups of informed individuals; each subgroup has a preferred direction of motion (representative of knowledge of location of food or migration route) that it can use to make decisions along with the information on its neighbors. It is shown in [3] that information can be transferred within groups even when there is no signaling, no identification of the informed individuals, and no evaluation of the information of individuals.

The model we propose and study in a simplified form in this paper corresponds to a deterministic set of ordinary differential equations. Each agent is modelled as a particle moving in the plane at constant speed with steering rate dependent on inter-particle measurements and possibly on prior information concerning preferred directions.

This model is similar to models used for cooperative control of engineered multi-agent systems. For instance, a continuous model of particles moving at constant speed in the plane with steering control (heading rate) designed to couple the dynamics of the particles has been used for stabilization of circular and parallel collective motion [4], [5]. The use of the same kinds of models in the engineered and natural settings is no accident. The very efficient way that animals move together and make collective decisions provides inspiration for design in engineering. Likewise, tools that have been developed for analysis and synthesis in the engineering context may prove useful for investigation in the natural setting. We note that the objectives

B. Nabet and N.E. Leonard were supported in part by ONR grants N00014–02–1–0861 and N00014–04–1–0534. I.D. Couzin acknowledges support from the Royal Society, Balliol College and EPSRC grants GR/S04765/01 and GR/T11234/01. S.A. Levin was supported in part by DARPA grant HR0011-05-1-0057 and NSF grant EF-0434319.

B. Nabet and N.E. Leonard are with the Department of Mechanical and Aerospace Engineering, Princeton University, Princeton, NJ, 08544 USA {bnabet,naomi}@princeton.edu.

I.D. Couzin is with the Department of Zoology, South Parks Road, University of Oxford, Oxford, OX1 3PS, UK iain.couzin@zoology.oxford.ac.uk

S.A. Levin is with the Department of Ecology and Evolutionary Biology, Princeton University, Princeton, NJ, 08544 USA slevin@princeton.edu

in engineering applications may be analogous to objectives in the natural setting. For example, in the design of mobile sensor networks (such as the autonomous ocean sampling network described in [6]), the goal is to maximize information intake. This has parallels with optimal social foraging, although under most biological circumstances grouping individuals are unrelated and thus perform selfishly, cooperative behavior being selected for only when it benefits individual reproductive success.

The central goal in the present work is to study the global phase space for the proposed simple model by computing equilibria and proving stability and bifurcations. Our planar particle model includes key features of the discrete model; however, for the purpose of analysis, it is made simpler. For example, as a first step we reduce the group to two informed subgroups, each with the same size population. We study bifurcations as a function of two bifurcation parameter: $K \geq 0$, the coupling gain that weights the attention paid to neighbors versus the preferred direction, and $\bar{\theta}_2 \in [0, \pi]$, the relative angle of the two preferred directions. In Section II, we present the general model and derive a reduced-order system. In Sections IV and V we study two specific choices for the parameters K and $\bar{\theta}_2$ for which we can find a closed-form expression for the equilibrium points and compute analytically the bifurcation diagrams. In Section VI we explain how the results change for unevenly sized groups of informed individuals and discuss future directions.

II. MODELS

We consider a population of N individuals with all-to-all coupling. This population is divided into three subgroups. Let N_1 and N_2 be the number of agents, respectively, in two different subgroups of informed individuals and let N_3 be the number of naive (uninformed) individuals such that $N_1 + N_2 + N_3 = N$. Let $\mathcal{N}_1$ and $\mathcal{N}_2$, respectively, be the set of indices corresponding to subgroups 1 and 2 which comprise the two different groups of informed individuals. Let $\mathcal{N}_3$ be the set of indices of the naive individuals. Then the cardinality of $\mathcal{N}_k$ is N_k, $k = 1, 2, 3$. The preferred heading direction for the individuals in $\mathcal{N}_i$ is denoted $\bar{\theta}_i$, for $i = 1, 2$.

We model each individual as a particle moving in the plane at constant speed. The heading direction of individual j is denoted θ_j, and θ_j is allowed to take any value in the circle S^1, for all j. Our simple model describes the dynamics of the heading angles for all individuals in the population. This model defines steering terms that depend only on relative heading angles. The model dynamics are given by

$$\begin{aligned}
\dot{\theta}_j &= \sin(\bar{\theta}_1 - \theta_j) + \frac{K}{N}\sum_{l=1}^{N}\sin(\theta_l - \theta_j), \quad j \in \mathcal{N}_1 \\
\dot{\theta}_j &= \sin(\bar{\theta}_2 - \theta_j) + \frac{K}{N}\sum_{l=1}^{N}\sin(\theta_l - \theta_j), \quad j \in \mathcal{N}_2 \\
\dot{\theta}_j &= \frac{K}{N}\sum_{l=1}^{N}\sin(\theta_l - \theta_j), \quad j \in \mathcal{N}_3\,. \qquad (1)
\end{aligned}$$

We note that the form of the coupling is based on the Kuramoto model for populations of coupled oscillators [7]. The model is also similar to that used by Mirollo and Strogatz to model a group of coupled spins in a random magnetic field [8]. In the coupled spin model, there are no subgroups; instead, each individual oscillator has a randomly assigned "pinning" angle $\bar{\theta}_j$ such that the pinning angles are uniformly distributed around the circle. The authors look at bifurcations as a function of K.

For each subgroup $k = 1, 2, 3$ we define the average phasor over all individuals in the subgroup as

$$\rho_k e^{i\psi_k} = \frac{1}{N_k}\sum_{j \in \mathcal{N}_k} e^{i\theta_j}.$$

The angle $\psi_k \in S^1$ defines the direction and $\rho_k \in [0, 1]$ the magnitude of the average phasor for the individuals in the kth subgroup for $k = 1, 2, 3$. In the case $K >> 1$ and N large, the large population model (1) has a separation of time scales. Individuals within each subgroup synchronize quickly, i.e., ρ_k quickly converges to 1 for $k = 1, 2, 3$. The slow dynamics are described by the following reduced system

$$\begin{aligned}
\dot{\psi}_1 &= \sin(\bar{\theta}_1 - \psi_1) + \frac{K}{N} \sum_{j=2,3} N_j \sin(\psi_j - \psi_1) \\
\dot{\psi}_2 &= \sin(\bar{\theta}_2 - \psi_2) + \frac{K}{N} \sum_{j=1,3} N_j \sin(\psi_j - \psi_2) \\
\dot{\psi}_3 &= \frac{K}{N} \sum_{j=1,2} N_j \sin(\psi_j - \psi_3). \qquad (2)
\end{aligned}$$

Here the three variables ψ_k characterize the lumped behavior of each of the three subgroups. Further details of the singular perturbation analysis will be reported in a future publication.

For the purposes of the bifurcation study in this paper, we consider the case in which $N_1 = N_2$ and $N_3 = 0$ such that (2) becomes

$$\begin{aligned}
\dot{\psi}_1 &= \sin(\bar{\theta}_1 - \psi_1) + \frac{K}{2} \sin(\psi_2 - \psi_1) \\
\dot{\psi}_2 &= \sin(\bar{\theta}_2 - \psi_2) + \frac{K}{2} \sin(\psi_1 - \psi_2). \qquad (3)
\end{aligned}$$

This model also appears to be the reduced model in the case $N_1 = N_2 \gg 1$ and $K \geq 0$ not necessarily large. Without loss of generality we set $\bar{\theta}_1 = 0$. The two bifurcation parameters are $K \geq 0$ and $\bar{\theta}_2 \in [0, \pi]$. We note that the general reduced system (2) is a gradient system. In the case of $N_1 = N_2$ and N_3, the gradient dynamics are

$$\dot{\psi}_k = -\frac{\partial V}{\partial \psi_k}, \qquad (4)$$

where V is given by

$$V = -\cos(\psi_1) - \cos(\bar{\theta}_2 - \psi_2) - \frac{K}{2} \cos(\psi_2 - \psi_1). \qquad (5)$$

Thus, by LaSalle's Invariance Principle, all solutions converge to the set of critical points of (5).

III. Equilibria

We first compute the equilibria of the system (3) but note that, in general, we cannot find closed form expressions for all of them. The equilibria are given by

$$\begin{aligned}
-\sin\psi_1 + \frac{K}{2} \sin(\psi_2 - \psi_1) = 0 \\
\sin(\bar{\theta}_2 - \psi_2) + \frac{K}{2} \sin(\psi_1 - \psi_2) = 0.
\end{aligned}$$

There are two sets of solutions, the first set given by

$$\begin{aligned}
\psi_1 &= \pi - \bar{\theta}_2 + \psi_2 \\
\sin(\psi_2 - \bar{\theta}_2) &= \frac{K}{2} \sin\bar{\theta}_2, \qquad (6)
\end{aligned}$$

and the second set given by

$$\begin{aligned}
\psi_1 &= \bar{\theta}_2 - \psi_2 \qquad (7) \\
\sin(\bar{\theta}_2 - \psi_2) &= \frac{K}{2} \sin(2\psi_2 - \bar{\theta}_2)\,. \qquad (8)
\end{aligned}$$

a) First set of solutions: Equation (6) has two solutions: $\psi_2 = \bar{\theta}_2 + \arcsin(\frac{K}{2}\sin\bar{\theta}_2)$ and $\psi_2 = \pi + \bar{\theta}_2 - \arcsin(\frac{K}{2}\sin\bar{\theta}_2)$. These two solutions exist if and only if $|\frac{K}{2}\sin\bar{\theta}_2| < 1$.

Lemma 3.1: If well defined, the two equilibria $\boldsymbol{\psi}_{S1} = (\psi_1, \psi_2)_{S1}$ and $\boldsymbol{\psi}_{S2} = (\psi_1, \psi_2)_{S2}$ satisfying (6) given by

$$\begin{aligned}
\boldsymbol{\psi}_{S1} &= \left(\pi + \arcsin\left(\frac{K}{2}\sin\bar{\theta}_2\right), \bar{\theta}_2 + \arcsin\left(\frac{K}{2}\sin\bar{\theta}_2\right)\right),\\
\boldsymbol{\psi}_{S2} &= \left(-\arcsin\left(\frac{K}{2}\sin\bar{\theta}_2\right), \pi + \bar{\theta}_2 - \arcsin\left(\frac{K}{2}\sin\bar{\theta}_2\right)\right),
\end{aligned}$$

are saddle points $\forall K > 0$ and $\forall \bar{\theta}_2 \in [0, \pi]$.

Proof: We look at the linearization of (3) at each of these two equilibria and show that its eigenvalues are always real and of opposite sign. The Jacobian of the system (3) is given by

$$J = \begin{pmatrix} -\cos\psi_1 - \frac{K}{2}\cos(\psi_2 - \psi_1) & \frac{K}{2}\cos(\psi_2 - \psi_1) \\ \frac{K}{2}\cos(\psi_2 - \psi_1) & -\cos(\bar{\theta}_2 - \psi_2) - \frac{K}{2}\cos(\psi_2 - \psi_1) \end{pmatrix}. \tag{9}$$

When we evaluate this matrix at either one of the two equilibria $\boldsymbol{\psi}_{S1}$ or $\boldsymbol{\psi}_{S2}$, we get

$$J|_{\boldsymbol{\psi}_{Si}} = \begin{pmatrix} \frac{K}{2}\cos\bar{\theta}_2 + \sqrt{1 - \frac{K^2}{4}\sin^2\bar{\theta}_2} & -\frac{K}{2}\cos\bar{\theta}_2 \\ -\frac{K}{2}\cos\bar{\theta}_2 & \frac{K}{2}\cos\bar{\theta}_2 - \sqrt{1 - \frac{K^2}{4}\sin^2\bar{\theta}_2} \end{pmatrix}.$$

Since the Jacobian is symmetric, the eigenvalues are real. The product of the two eigenvalues is

$$\lambda_1\lambda_2 = \frac{K^2}{4}\sin^2\bar{\theta}_2 - 1 < 0 \quad \text{for} \quad \left|\frac{K}{2}\sin\bar{\theta}_2\right| < 1.$$

Therefore, for $\bar{\theta}_2 \in [0, \pi]$ the eigenvalues of the linearization are real and of opposite sign. This implies that equilibria $\boldsymbol{\psi}_{S1}$ and $\boldsymbol{\psi}_{S2}$, if well defined, are saddle points $\forall K > 0$ and $\forall \bar{\theta}_2 \in [0, \pi]$. $\square$

b) Second set of solutions: In order to study (7)-(8 we make a change of variables $(\psi_1, \psi_2) \mapsto (\rho, \Psi)$ where $\rho \in [0, 1]$ and $\Psi \in S^1$ and we define

$$\rho e^{i\Psi} = \frac{1}{2}(e^{i\psi_1} + e^{i\psi_2}).$$

Expanding this out and using (7) we compute

$$\begin{aligned}
\rho(\cos(\Psi) + i\sin(\Psi)) &= \frac{1}{2}(\cos(\psi_1) + \cos(\psi_2)) + \frac{1}{2}i(\sin(\psi_1) + \sin(\psi_2))\\
&= \cos\left(\frac{\psi_1 - \psi_2}{2}\right)\cos\left(\frac{\psi_1 + \psi_2}{2}\right) + i\cos\left(\frac{\psi_1 - \psi_2}{2}\right)\sin\left(\frac{\psi_1 + \psi_2}{2}\right)\\
&= \cos\left(\frac{\bar{\theta}_2}{2} - \psi_2\right)\left(\cos\left(\frac{\bar{\theta}_2}{2}\right) + i\sin\left(\frac{\bar{\theta}_2}{2}\right)\right).
\end{aligned} \tag{10}$$

For $\bar{\theta}_2 \in [0, \pi]$, (10) implies that $\Psi = \frac{\bar{\theta}_2}{2}$ or $\Psi = \frac{\bar{\theta}_2}{2} + \pi$. We can rewrite (8) as

$$\sin\frac{\bar{\theta}_2}{2}\cos\left(\frac{\bar{\theta}_2}{2} - \psi_2\right) + \cos\frac{\bar{\theta}_2}{2}\sin\left(\frac{\bar{\theta}_2}{2} - \psi_2\right) + K\sin\left(\frac{\bar{\theta}_2}{2} - \psi_2\right)\cos\left(\frac{\bar{\theta}_2}{2} - \psi_2\right) = 0. \tag{11}$$

In Section V we study the special case $\bar{\theta}_2 = \pi$. Here we focus on $\bar{\theta}_2 \in [0, \pi)$.

For $\Psi = \frac{\bar{\theta}_2}{2}$, (10) implies that $\cos(\frac{\bar{\theta}_2}{2} - \psi_2) = \rho$ and $\sin(\frac{\bar{\theta}_2}{2} - \psi_2) \pm \sqrt{1 - \rho^2}$. Accordingly, (11) implies that ρ satisfies

$$\rho\sin\frac{\bar{\theta}_2}{2} + \sqrt{1 - \rho^2}\cos\frac{\bar{\theta}_2}{2} + K\rho\sqrt{1 - \rho^2} = 0 \tag{12}$$

or

$$\rho \sin \frac{\bar{\theta}_2}{2} - \sqrt{1-\rho^2} \cos \frac{\bar{\theta}_2}{2} - K\rho\sqrt{1-\rho^2} = 0. \tag{13}$$

We get that $\rho = 1$ if and only if $\bar{\theta}_2 = 0$ and $\rho = 0$ if and only if $\bar{\theta}_2 = \pi$. For $\bar{\theta}_2 \in (0, \pi)$, equation (12) does not have any solution for $\rho \in (0,1)$ since every term on the left is positive, and equation (13) has one solution for $\rho \in (0,1)$. We call the corresponding equilibrium $\boldsymbol{\psi}_{sync1} := (\psi_1, \psi_2)_{sync1}$.

Lemma 3.2: The equilibrium $\boldsymbol{\psi}_{sync1}$ is a stable node for all $(K, \bar{\theta}_2) \in [0, \infty) \times [0, \pi)$.

Proof In order to prove this result, we show that the Jacobian has both eigenvalues real and negative. Using $\cos(\frac{\bar{\theta}_2}{2} - \psi_2) = \rho$ and $\sin(\frac{\bar{\theta}_2}{2} - \psi_2) = -\sqrt{1-\rho^2}$ we can write the Jacobian evaluated at this equilibrium as

$$J|_{\boldsymbol{\psi}_{sync1}} = \begin{pmatrix} -(\rho \cos \frac{\bar{\theta}_2}{2} + \sqrt{1-\rho^2} \sin \frac{\bar{\theta}_2}{2} + \frac{K}{2}(2\rho^2 - 1)) & \frac{K}{2}(2\rho^2-1) \\ \frac{K}{2}(2\rho^2-1) & -(\rho \cos \frac{\bar{\theta}_2}{2} + \sqrt{1-\rho^2} \sin \frac{\bar{\theta}_2}{2} + \frac{K}{2}(2\rho^2 - 1)) \end{pmatrix}.$$

Since the diagonal matrix elements are equal and the off diagonal elements are equal, the eigenvalues are the sum and difference of these elements:

$$\lambda_{1,2} = -(\rho \cos \frac{\bar{\theta}_2}{2} + \sqrt{1-\rho^2} \sin \frac{\bar{\theta}_2}{2} + \frac{K}{2}(2\rho^2-1)) \pm \frac{K}{2}(2\rho^2 - 1).$$

We find using (13) for all $(K, \bar{\theta}_2) \in [0, \infty) \times [0, \pi)$ that

$$-\sqrt{1-\rho^2} \sin \frac{\bar{\theta}_2}{2} - K(2\rho^2 - 1) = \sqrt{1-\rho^2} \sin \frac{\bar{\theta}_2}{2} - \frac{2}{\rho}(1-\rho^2) \cos \frac{\bar{\theta}_2}{2} - 1 < 0. \tag{14}$$

Thus, for all $(K, \bar{\theta}_2) \in [0, \infty) \times [0, \pi)$, using (14) both eigenvalues are real and negative. Hence $\boldsymbol{\psi}_{sync1}$ is a stable node for all $(K, \bar{\theta}_2) \in [0, \infty) \times [0, \pi)$. $\square$

For $\Psi = \frac{\bar{\theta}_2}{2} + \pi$, (10) implies that $\cos(\frac{\bar{\theta}_2}{2} - \psi_2) = -\rho$ and $\sin(\frac{\bar{\theta}_2}{2} - \psi_2) = \pm\sqrt{1-\rho^2}$. Hence, by (11) ρ has to satisfy

$$-\rho \sin \frac{\bar{\theta}_2}{2} + \sqrt{1-\rho^2} \cos \frac{\bar{\theta}_2}{2} - K\rho\sqrt{1-\rho^2} = 0 \tag{15}$$

or

$$-\rho \sin \frac{\bar{\theta}_2}{2} - \sqrt{1-\rho^2} \cos \frac{\bar{\theta}_2}{2} + K\rho\sqrt{1-\rho^2} = 0. \tag{16}$$

Equation (15) has one solution for $\rho \in [0,1]$, we call the corresponding equilibrium $\boldsymbol{\psi}_{antisync1} := (\psi_1, \psi_2)_{antisync1}$.

Lemma 3.3: The equilibrium $\boldsymbol{\psi}_{antisync1}$ is unstable for all $(K, \bar{\theta}_2) \in [0, \infty) \times [0, \pi)$.

Proof In order to prove this result, we show that the Jacobian has at least one real, positive eigenvalue. Using $\cos(\frac{\bar{\theta}_2}{2} - \psi_2) = -\rho$ and $\sin(\frac{\bar{\theta}_2}{2} - \psi_2) = \sqrt{1-\rho^2}$ we can write the Jacobian evaluated at this equilibrium as

$$J|_{\boldsymbol{\psi}_{antisync1}} = \begin{pmatrix} \rho \cos \frac{\bar{\theta}_2}{2} + \sqrt{1-\rho^2} \sin \frac{\bar{\theta}_2}{2} - \frac{K}{2}(2\rho^2 - 1) & \frac{K}{2}(2\rho^2-1) \\ \frac{K}{2}(2\rho^2-1) & \rho \cos \frac{\bar{\theta}_2}{2} + \sqrt{1-\rho^2} \sin \frac{\bar{\theta}_2}{2} - \frac{K}{2}(2\rho^2 - 1) \end{pmatrix}.$$

The matrix has the same symmetry as in Lemma 3.2 and the eigenvalues can easily be computed to be

$$\lambda_{1,2} = \rho \cos \frac{\bar{\theta}_2}{2} + \sqrt{1-\rho^2} \sin \frac{\bar{\theta}_2}{2} - \frac{K}{2}(2\rho^2-1) \pm \frac{K}{2}(2\rho^2 - 1).$$

One eigenvalue is equal to $\rho \cos \frac{\bar{\theta}_2}{2} + \sqrt{1-\rho^2} \sin \frac{\bar{\theta}_2}{2} > 0$ for all $(K, \bar{\theta}_2) \in [0, \infty) \times [0, \pi)$. Hence $\boldsymbol{\psi}_{antisync1}$ is unstable for all $(K, \bar{\theta}_2) \in [0, \infty) \times [0, \pi)$. $\square$

Equation (16) has zero or two solutions for $\rho \in [0,1]$, although we are not able to find analytically the range of parameters in which there are solutions nor the nature of their stability. The equilibria we get from (16) will be called $\boldsymbol{\psi}_{sync2} := (\psi_1, \psi_2)_{sync2}$ and $\boldsymbol{\psi}_{antisync2} := (\psi_1, \psi_2)_{antisync2}$.

For all solutions (of the second set), in equations (13), (15) and (16), as K gets increasingly large, $K\rho\sqrt{1-\rho^2}$ must approach zero. This means that as $K\to\infty$ then $\rho\to 0$ or $\rho\to 1$. We call an equilibrium *synchronized* if ψ_1 and ψ_2 are the same heading and *anti-synchronized* if the relative heading between ψ_1 and ψ_2 is equal to π. Thus, for very large values of K all the equilibria will be either *synchronized* or *anti-synchronized*. For modest values of K, the strength of the coupling is less than or equal to the strength of the attraction to the preferred direction, and the equilibria are typically neither fully synchronized nor fully anti-synchronized. In this case we call an equilibrium K-*almost synchronized* (K-*almost anti-synchronized*) if the corresponding equilibrium in the case $K \gg 1$, is synchronized (anti-synchronized). As we showed, almost synchronization occurs at $\Psi = \frac{\bar{\theta}_2}{2}$ and $\Psi = \frac{\bar{\theta}_2}{2} + \pi$. Note that these correspond to an exact compromise between the two preferred directions.

Figures 1 shows a bifurcation diagram in the cases $\bar{\theta}_2 = 1$ rad and $\bar{\theta}_2 = 2$ rad. The bifurcation parameter is K and ρ is plotted as a function of K for all equilibria in the second set of solutions. We see that there are two equilibria that do not exist for some values of K; these two equilibria come from (16). We also note in comparing Figures 1 (a) and (b) that the stability of these equilibria changes as a function of K and $\bar{\theta}_2$. This indicates the presence of bifurcations. There are two other equilibria that are defined for all values of K. The stable node is $\boldsymbol{\psi}_{sync1}$ which comes from (13). This equilibrium becomes synchronized as K increases, i.e., $\rho\to 1$ as $K\to\infty$. The unstable node is $\boldsymbol{\psi}_{antisync1}$ which comes from (15). This equilibrium becomes anti-synchronized as K increases, i.e., $\rho\to 0$ as $K\to\infty$. It can be seen that as K increases ρ approaches 0 or 1 also for the two other equilibria. The fact that for large values of K, all the equilibria in this set become either synchronized or anti-synchronized is due to the term $K\rho\sqrt{1-\rho^2}$ in (13)-(15) and (16).

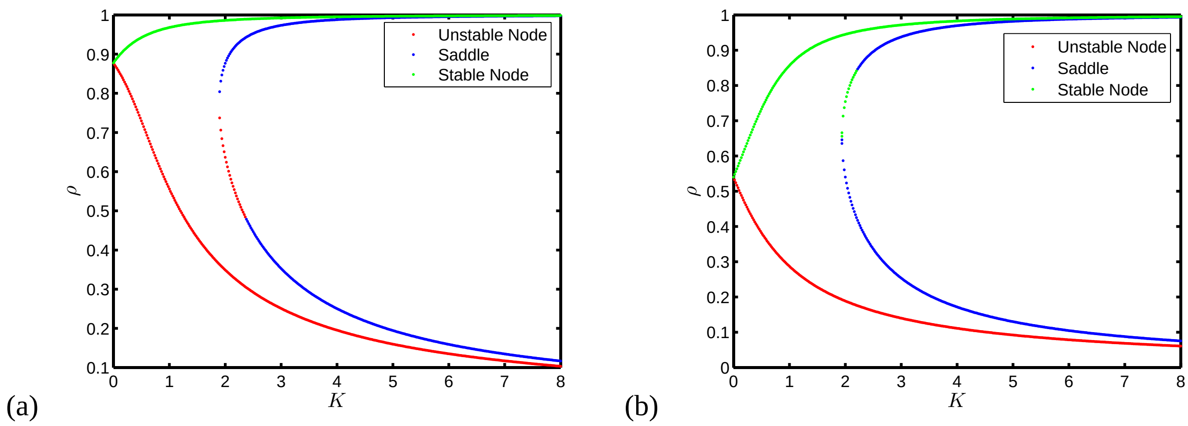

Fig. 1. Bifurcation diagrams in cases (a) $\bar{\theta}_2 = 1$ rad and (b) $\bar{\theta}_2 = 2$ rad. The bifurcation parameter is K and ρ is plotted as a function of K for all equilibria in the second set of solutions. We note that two equilibria do not exist for some values of K. Stability of these same two equilibria changes type between (a) and (b). This indicates the presence of bifurcations.

IV. Analytically solvable case fixing $K = 2$

In this section we set $K = 2$ and study the bifurcations in the $(\bar{\theta}_2, \psi_i)$ plane. In this case, the strength of the attraction towards the preferred direction is equal to the strength of the attraction to align with the other subgroup.

The system (3) now becomes

$$\begin{aligned} \dot{\psi}_1 &= -\sin\psi_1 + \sin(\psi_2 - \psi_1) \\ \dot{\psi}_2 &= \sin(\bar{\theta}_2 - \psi_2) - \sin(\psi_2 - \psi_1). \end{aligned} \tag{17}$$

A. Equilibria of the system

For $K = 2$, (8) becomes $\sin(\bar{\theta}_2 - \psi_2) = \sin(2\psi_2 - \bar{\theta}_2)$. This equation has four solutions,

$$\psi_2 = \begin{cases} \frac{2}{3}\bar{\theta}_2 \\ \frac{2}{3}\bar{\theta}_2 + \frac{2\pi}{3} \\ \frac{2}{3}\bar{\theta}_2 + \frac{4\pi}{3} \\ \pi. \end{cases}$$

The system therefore has a total of six equilibria given by

- Eq1: $\boldsymbol{\psi}_{sync1} = (\frac{1}{3}\bar{\theta}_2, \frac{2}{3}\bar{\theta}_2)$

  Using Lemma 3.2 we know that $\boldsymbol{\psi}_{sync1}$ is a *stable node* for $\bar{\theta}_2 \in [0, \pi]$.

- Eq2: $\boldsymbol{\psi}_{sync2} = (\frac{1}{3}\bar{\theta}_2 - \frac{2\pi}{3}, \frac{2}{3}\bar{\theta}_2 + \frac{2\pi}{3})$

  The Jacobian of the system evaluated at this equilibrium is $J = \cos(\frac{1}{3}\bar{\theta}_2 - \frac{2\pi}{3}) \begin{pmatrix} -2 & 1 \\ 1 & -2 \end{pmatrix}$. The eigenvalues of this matrix are $\{-\cos(\frac{1}{3}\bar{\theta}_2 - \frac{2\pi}{3}), -3\cos(\frac{1}{3}\bar{\theta}_2 - \frac{2\pi}{3})\}$. Both eigenvalues are strictly positive for $\bar{\theta}_2 \in [0, \frac{\pi}{2})$, and both strictly negative for $\bar{\theta}_2 \in (\frac{\pi}{2}, \pi]$. So the equilibrium $\boldsymbol{\psi}_{sync2}$ is an *unstable node* for $\bar{\theta}_2 \in [0, \frac{\pi}{2})$ and a *stable node* for $\bar{\theta}_2 \in (\frac{\pi}{2}, \pi]$.

- Eq3: $\boldsymbol{\psi}_{antisync1} = (\frac{1}{3}\bar{\theta}_2 - \frac{4\pi}{3}, \frac{2}{3}\bar{\theta}_2 + \frac{4\pi}{3})$

  Using Lemma 3.3 we know that the equilibrium $\boldsymbol{\psi}_{antisync1}$ is an *unstable node* for $\bar{\theta}_2 \in [0, \pi]$.

- Eq4: $\boldsymbol{\psi}_{antisync2} = (\bar{\theta}_2 - \pi, \pi)$

  The Jacobian of the system evaluated at this equilibrium is $J = \cos\bar{\theta}_2 \begin{pmatrix} 0 & 1 \\ 1 & 0 \end{pmatrix}$. The eigenvalues of this matrix are $\{-\cos\bar{\theta}_2, \cos\bar{\theta}_2\}$ which are of opposite sign for all $\bar{\theta}_2 \in [0, \frac{\pi}{2}) \cup (\frac{\pi}{2}, \pi]$. So the equilibrium $\boldsymbol{\psi}_{antisync2}$ is a *saddle point* for $\bar{\theta}_2 \in [0, \frac{\pi}{2}) \cup (\frac{\pi}{2}, \pi]$.

- Eq5: $\boldsymbol{\psi}_{S1} = (\bar{\theta}_2 + \pi, 2\bar{\theta}_2)$

  Using Lemma 3.1 we know that $\boldsymbol{\psi}_{S1}$ is a *saddle point* for all $\bar{\theta}_2 \in [0, \frac{\pi}{2}) \cup (\frac{\pi}{2}, \pi]$.

- Eq6: $\boldsymbol{\psi}_{S2} = (-\bar{\theta}_2, \pi)$

  Using Lemma 3.1 we know that $\boldsymbol{\psi}_{S2}$ is a *saddle point* for all $\bar{\theta}_2 \in [0, \frac{\pi}{2}) \cup (\frac{\pi}{2}, \pi]$.

Figure 2 shows an example of the six equilibria in the case $\bar{\theta}_2 = 1$ rad.

B. Analysis of the bifurcation diagram:

Using the analysis of the previous subsection, we can see that the stability type of one of the equilibria, $\boldsymbol{\psi}_{sync2}$, changes at $\bar{\theta}_2 = \frac{\pi}{2}$ from an unstable node to a stable node. When we look closer at $\boldsymbol{\psi}_{sync2}$ for $\bar{\theta}_2 = \frac{\pi}{2}$, we see that it is a highly degenerate equilibrium; the linearization J is equal to the zero matrix. Figure 3 shows the bifurcation diagram in the $(\bar{\theta}_2, \psi_1)$ plane, i.e, ψ_1 as a function of bifurcation parameter $\bar{\theta}_2$. The bifurcation diagram in the $(\bar{\theta}_2, \psi_2)$ plane looks similar. In the bifurcation diagram (Figure 3) we see that four equilibria come together at the point in phase space $(\psi_1, \psi_2) = (\frac{3\pi}{2}, \pi)$ when $\bar{\theta}_2 = \frac{\pi}{2}$. This bifurcation is one of the seven of Thom's elementary catastrophes; it is called the *elliptic umbilic* [9].

Catastrophe theory applies to gradient systems, and the elementary catastrophes are classified by looking at the form of the potential. As previously mentioned, our system obeys gradient dynamics and the associated potential for $K = 2$ is

$$V = \cos(\psi_1) + \cos(\bar{\theta}_2 - \psi_2) + \cos(\psi_1 - \psi_2). \tag{18}$$

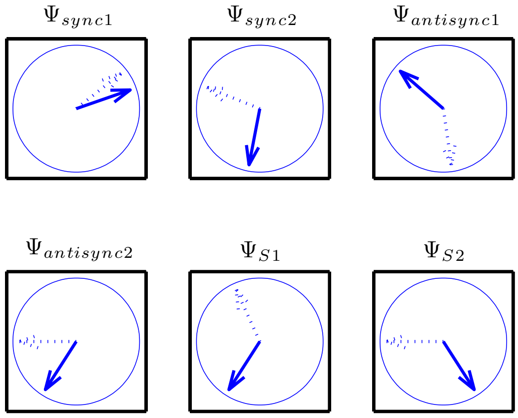

Fig. 2. Picture of the six equilibria for $K = 2$ and $\bar{\theta}_2 = 1$ rad. The solid arrow represents ψ_1 on the unit circle, i.e., the average heading of the first informed subgroup, and the dashed arrow represents ψ_2, the average heading of the second informed subgroup.

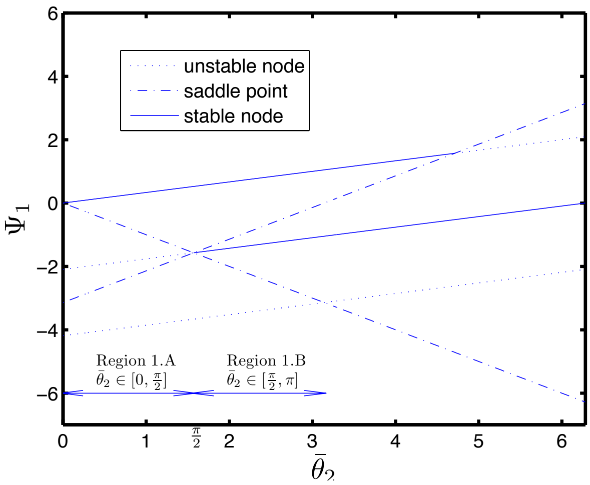

Fig. 3. Bifurcation diagram in the $(\bar{\theta}_2, \psi_1)$ plane, i.e, ψ_1 as a function of bifurcation parameter $\bar{\theta}_2$ fixing $K = 2$. Since the equilibria $\boldsymbol{\psi}_{antisync2}$ and $\boldsymbol{\psi}_{S1}$ have the same value for ψ_1 (but a different value for ψ_2), we see on this diagram only five equilibria even though there are six. At $\bar{\theta}_2 = \frac{\pi}{2}$ there are only three distinct equilibria; this is the degenerate point of the system. The multiplicity of the equilibrium $(\frac{3\pi}{2}, \pi)$ is four.

To identify the bifurcation as an elliptic umbilic, we look at the unfolding of this potential near the catastrophe $(\psi_1, \psi_2, \bar{\theta}_2) = (\frac{3\pi}{2}, \pi, \frac{\pi}{2})$. We write (18) as

$$V = \cos(u + \frac{3\pi}{2}) + \cos(\frac{\pi}{2} + a - (\pi + v)) + \cos(u + \frac{3\pi}{2} - (\pi + v)), \tag{19}$$

where u and v are respectively the deviation of ψ_1 from $\frac{3\pi}{2}$ and ψ_2 from π, and a the deviation of $\bar{\theta}_2$ from $\frac{\pi}{2}$. We do a Taylor expansion of (19), keeping terms up to third order in u and v, and get

$$V = \frac{(\cos(a) - 1)}{3!}v^3 + \frac{uv^2}{2} - \frac{vu^2}{2} - \frac{\sin(a)}{2}v^2 + (1 - \cos(a))v + \sin(a). \tag{20}$$

We now make the following change of variable:

$$
\begin{aligned}
x &= \frac{1}{2}\sqrt[3]{\frac{(4\cos(a)-1)}{3}}\,v \\
y &= \sqrt[3]{\frac{2\sqrt{6}}{\sqrt{4\cos(a)-1}}}\left(\frac{1}{\sqrt{6}}u - \frac{1}{2\sqrt{6}}v\right),
\end{aligned}
$$

and get for the potential

$$
V = x^3 - 3xy^2 - \frac{2\times 3^{\frac{2}{3}}\sin(a)}{(4\cos(a)-1)^{\frac{2}{3}}}x^2 - \frac{2\times 3^{\frac{1}{3}}(\cos(a)-1)}{(4\cos(a)-1)^{\frac{1}{3}}}x + \sin(a). \tag{21}
$$

In (21) we recognize the standard unfolding of the potential of an elliptic umbilic [10].

In the following paragraph we examine the different equilibria in each of the various regions of the bifurcation diagram. Region 1.A is defined by $\bar{\theta}_2 \in [0, \frac{\pi}{2}]$ and Region 1.B by $\bar{\theta}_2 \in (\frac{\pi}{2}, \pi]$. For each case studied, we draw the pictures of each possible equilibrium (stable and unstable) on the unit circle, a solid arrow corresponding to ψ_1 and a dashed arrow corresponding to ψ_2. Because $K = 2$ implies equal strength of the coupling as compared to the preferred direction, equilibria are usually not fully synchronized nor anti-synchronized; the equilibria $\boldsymbol{\psi}_{sync1}$, $\boldsymbol{\psi}_{sync2}$, $\boldsymbol{\psi}_{antisync1}$ and $\boldsymbol{\psi}_{antisync2}$ are *K-almost synchronized* or *K-almost anti-synchronized*. Since $\boldsymbol{\psi}_{S1}$ and $\boldsymbol{\psi}_{S2}$ from (6) are not defined for $K \gg 1$, we cannot use this terminology. However, we note that the relative heading of ψ_1 and ψ_2 is always equal to $\pi - \bar{\theta}_2$ for $\boldsymbol{\psi}_{S1}$ and $\pi + \bar{\theta}_2$ for $\boldsymbol{\psi}_{S2}$. As $\bar{\theta}_2$ increases to π, the two saddles become synchronized. We call an equilibrium *$\bar{\theta}_2$-almost synchronized* if the corresponding equilibrium in the case $\bar{\theta}_2 \to \pi$ is synchronized.

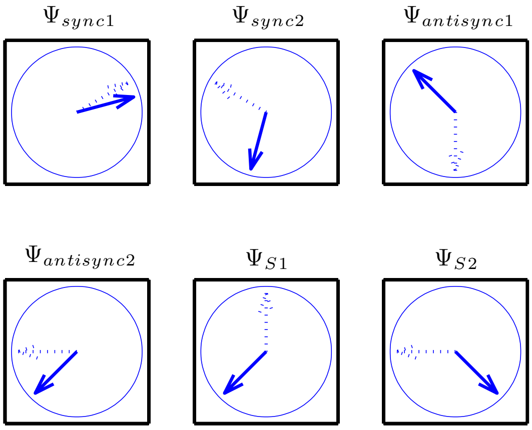

Fig. 4. These diagrams show pictures of all the equilibria for $\bar{\theta}_2 = \frac{\pi}{4}$. This is representative of the possible equilibria for the system in Region 1A without its boundary, i.e., for $\bar{\theta}_2 \in [0, \frac{\pi}{2})$. The only stable equilibrium is ψ_{sync1} which corresponds to the motion with $\Psi = \frac{\pi}{8}$ direction.

Region 1.A $\bar{\theta}_2 \in [0, \frac{\pi}{2}]$. The equilibria in the case $\bar{\theta}_2 \in [0, \frac{\pi}{2})$ are shown in Figure 4. Figure 5 shows the equilibria at the bifurcation point $\bar{\theta}_2 = \frac{\pi}{2}$. In Figure 4 we see that there are three types of equilibria: the K-almost synchronized $\boldsymbol{\psi}_{sync1}$ and $\boldsymbol{\psi}_{sync2}$, the K-almost anti-synchronized $\boldsymbol{\psi}_{antisync1}$ and $\boldsymbol{\psi}_{antisync2}$ and the $\bar{\theta}_2$-almost synchronized $\boldsymbol{\psi}_{S1}$ and $\boldsymbol{\psi}_{S2}$. The only stable equilibrium, $\boldsymbol{\psi}_{sync1}$, is the K-almost synchronized motion of ψ_1 and ψ_2 in the direction $\Psi = \frac{\bar{\theta}_2}{2}$ with each heading remaining on its side (nearest its preferred direction) of $\Psi = \frac{\bar{\theta}_2}{2}$. The unstable equilibria are the two K-almost anti-synchronized $\boldsymbol{\psi}_{antisync1}$ and $\boldsymbol{\psi}_{antisync2}$, the remaining K-almost synchronized $\boldsymbol{\psi}_{sync2}$ which flanks $\Psi = \frac{\bar{\theta}_2}{2} + \pi$ and the two $\bar{\theta}_2$-almost synchronized

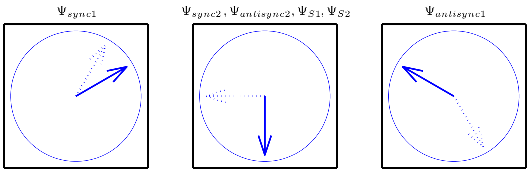

Fig. 5. These diagrams show the equilibria of the system at the critical point, i.e when both $K = 2$ and $\bar{\theta}_2 = \frac{\pi}{2}$. We only have three equilibria. The second equilibrium drawn is the superposition of four equilibria ψ_{sync2}, $\psi_{antisync2}$, ψ_{S1} and ψ_{S2}; it has multiplicity four. It is called a monkey-saddle in the catastrophe theory literature.

saddles. The first saddle ψ_{S1} is closer to the preferred direction $\bar{\theta}_1 = 0$, and the second saddle ψ_{S2} is closer to $\bar{\theta}_2$.

As mentioned previously, the case at the boundary $\bar{\theta}_2 = \frac{\pi}{2}$ is highly degenerate. There are only three distinct equilibria. We still have only one stable equilibrium which is K-almost synchronized at $\Psi = \frac{\bar{\theta}_2}{2} = \frac{\pi}{4}$. There is also an unstable K-almost anti-synchronized equilibrium $\psi_{antisync1}$ at $\Psi = \frac{\bar{\theta}_2}{2} + \pi = \frac{5\pi}{4}$. The other equilibrium corresponds to $\Psi = \frac{\bar{\theta}_2}{2} + \pi = \frac{5\pi}{4}$. When we look at the bifurcation diagram, we see that it is the superposition of four equilibria ψ_{sync2}, ψ_{S1}, ψ_{S2} and $\psi_{antisync2}$. This equilibrium is called a *monkey-saddle* in the catastrophe theory literature [10]

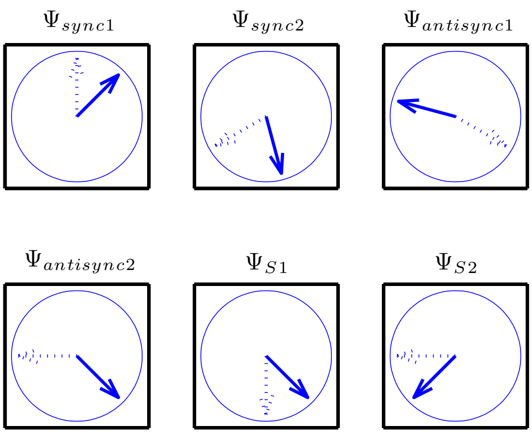

Fig. 6. These diagrams show the pictures of all the equilibria for $\bar{\theta}_2 = \frac{3\pi}{4}$. This is representative of the possible equilibria for the system in Region 1B without its boundary i.e for $\bar{\theta}_2 \in (\frac{\pi}{2}, \pi)$. The two saddles, ψ_{S1} and ψ_{S2} tend to be more synchronized (than in Figure 4) since $\bar{\theta}_2$ is closer to π. ψ_{S1} is closer to the preferred direction of the first subgroup and ψ_{S2} is closer to the preferred direction of the second subgroup. There are two stable equilibria, ψ_{sync1} and ψ_{sync2}.

Region 1.B $\bar{\theta}_2 \in (\frac{\pi}{2}, \pi]$. The equilibria in the case $\bar{\theta}_2 \in (\frac{\pi}{2}, \pi)$ are shown in Figure 6. Figure 7 shows the equilibria at the boundary $\bar{\theta}_2 = \pi$. In Figure 6 the equilibria we have are similar to those from the case where $\bar{\theta}_2 \in [0, \frac{\pi}{2})$ in Figure 4 except that now the K-almost synchronized equilibrium ψ_{sync2} at $\frac{\bar{\theta}_2}{2} + \pi$ is

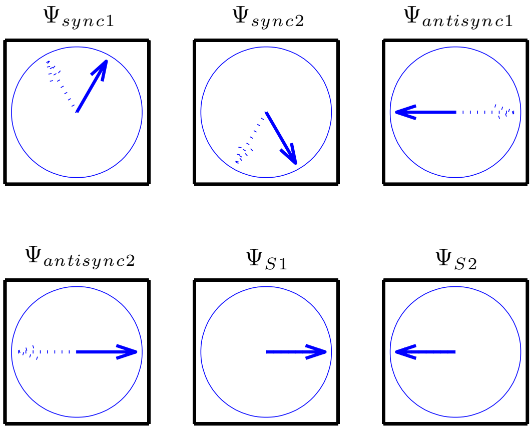

Fig. 7. These diagrams show the equilibria of the system at the right boundary of Region 1.B, i.e., for $\bar{\theta}_2 = \pi$. Only equilibrium $\boldsymbol{\psi}_{sync1}$ and $\boldsymbol{\psi}_{sync2}$ (the K-almost synchronized equilibria) depend on K. The other equilibria are anti-synchronized ($\boldsymbol{\psi}_{antisync1}$ and $\boldsymbol{\psi}_{antisync2}$) or synchronized ($\boldsymbol{\psi}_{S1}$ and $\boldsymbol{\psi}_{S2}$) for all K.

stable. Two of the unstable equilibria ($\boldsymbol{\psi}_{antisync1}$,$\boldsymbol{\psi}_{antisync2}$) are K-almost anti-synchronized. As mentioned above, for $\boldsymbol{\psi}_{S1}$ and $\boldsymbol{\psi}_{S2}$, the particles synchronize as $\bar{\theta}_2$ increases; the saddle $\boldsymbol{\psi}_{S1}$ is closer to the preferred direction of the first particle and the saddle $\boldsymbol{\psi}_{S2}$ is closer to the preferred direction of the second particle.

When looking at the case $\bar{\theta}_2 = \pi$, we still have two stable equilibria ($\boldsymbol{\psi}_{sync1}$,$\boldsymbol{\psi}_{sync2}$) which are K-almost synchronized at $\Psi = \frac{\bar{\theta}_2}{2} = \frac{\pi}{2}$ and $\Psi = \frac{\bar{\theta}_2}{2} + \pi = \frac{3\pi}{2}$. The unstable equilibria $\boldsymbol{\psi}_{antisync1}$ and $\boldsymbol{\psi}_{antisync2}$ are anti-synchronized. The two saddles are synchronized; $\boldsymbol{\psi}_{S1}$ is synchronized at the preferred direction of the first particle ($\bar{\theta}_1 = 0$) and $\boldsymbol{\psi}_{S2}$ is synchronized at the preferred direction of the second particle ($\bar{\theta}_2 = \pi$).

V. Analytically solvable case fixing $\bar{\theta}_2 = \pi$

In this section, we set $\bar{\theta}_2 = \pi$, and study the bifurcation in the (K, ψ_i) plane. For this case, the two preferred headings differ by 180 degrees. For this value of $\bar{\theta}_2$, the disagreement is so large that in some range of K the group will split without making any compromise; this kind of splitting is sometimes observed in swarm-bees [11]. The system (3) now becomes

$$\begin{aligned} \dot{\psi}_1 &= -\sin\psi_1 + \frac{K}{2}\sin(\psi_2 - \psi_1) \\ \dot{\psi}_2 &= \sin\psi_2 + \frac{K}{2}\sin(\psi_1 - \psi_2). \end{aligned} \tag{22}$$

We note that this system appears in chapter 8 of [12].

A. Equilibria of the system

The equation (8) now becomes $\sin\psi_2 = -\frac{K}{2}\sin 2\psi_2$. After some trigonometric manipulation we can rewrite this equation as

$$\sin\psi_2(1 + K\cos\psi_2) = 0. \tag{23}$$

We consider first the case that $K \in [0, 1)$. In this case equation (23) has two solutions

$$\psi_2 = \begin{cases} 0 \\ \pi. \end{cases}$$

This give us a total of four equilibria given by

- Eq1: $\boldsymbol{\psi}_{antisync1} = (\pi, 0)$

Using Lemma 3.3 we know that the equilibrium $\boldsymbol{\psi}_{antisync1}$ is an *unstable node* for $K \in [0,1]$.

- Eq2: $\boldsymbol{\psi}_{antisync2} = (0,\pi)$

  The Jacobian of the system evaluated at this equilibrium is $J = \begin{pmatrix} -1+\frac{K}{2} & -\frac{K}{2} \\ -\frac{K}{2} & -1+\frac{K}{2} \end{pmatrix}$. The eigenvalues of this matrix are $\{-1, -1+K\}$. Hence the linearization has both eigenvalues strictly negative $\forall K \in [0,1)$. So the equilibrium $\boldsymbol{\psi}_{antisync2}$ is a *stable node* $\forall K \in [0,1)$.

- Eq3: $\boldsymbol{\psi}_{S1} = (0,0)$

  Using Lemma 3.1 we know that $\boldsymbol{\psi}_{S1}$ is a *saddle point* for all $K \in [0,1]$.

- Eq4: $\boldsymbol{\psi}_{S2} = (\pi,\pi)$

  Using Lemma 3.1 we know that $\boldsymbol{\psi}_{S2}$ is a *saddle point* for all $K \in [0,1]$.

We consider next the case that $K > 1$. Equation (23), in this case has four solutions

$$\psi_2 = \begin{cases} \arccos(-\frac{1}{K}) \\ -\arccos(-\frac{1}{K}) \\ 0 \\ \pi. \end{cases}$$

We have now a total of six equilibria given by

- Eq1: $\boldsymbol{\psi}_{sync1} = (\pi - \arccos(-\frac{1}{K}), \arccos(-\frac{1}{K}))$

  Using Lemma 3.2 we know that $\boldsymbol{\psi}_{sync1}$ is a *stable node* for $K > 1$.

- Eq2: $\boldsymbol{\psi}_{sync2} = (\pi + \arccos(-\frac{1}{K}), -\arccos(-\frac{1}{K}))$

  The Jacobian of the system evaluated at this equilibrium is $J = \begin{pmatrix} -\frac{K}{2} & -\frac{1}{K}+\frac{K}{2} \\ -\frac{1}{K}+\frac{K}{2} & -\frac{K}{2} \end{pmatrix}$. The eigenvalues of this matrix are $\{-\frac{1}{K}, \frac{1-K^2}{K}\}$. hence the linearization has both eigenvalues strictly negative $\forall K > 1$. So the equilibrium $\boldsymbol{\psi}_{sync2}$ is a *stable node* $\forall K > 1$.

- Eq3: $\boldsymbol{\psi}_{antisync1} = (\pi, 0)$

  Using Lemma 3.3 we know that the equilibrium $\boldsymbol{\psi}_{antisync1}$ is an *unstable node* for $K \geq 1$.

- Eq4: $\boldsymbol{\psi}_{antisync2} = (0,\pi)$

  The Jacobian of the system evaluated at this equilibrium is $J = \begin{pmatrix} -1+\frac{K}{2} & -\frac{K}{2} \\ -\frac{K}{2} & -1+\frac{K}{2} \end{pmatrix}$. The eigenvalues of this matrix are $\{-1, -1+K\}$. Hence the linearization has its eigenvalues of opposite sign $\forall K > 1$. So the equilibrium $\boldsymbol{\psi}_{antisync2}$ is a *saddle point* $\forall K > 1$.

- Eq5: $\boldsymbol{\psi}_{S1} = (0,0)$

  Using Lemma 3.1 we know that $\boldsymbol{\psi}_{S1}$ is a *saddle point* for all $K \geq 1$.

- Eq6: $\boldsymbol{\psi}_{S2} = (\pi,\pi)$

  Using Lemma 3.1 we know that $\boldsymbol{\psi}_{S2}$ is a *saddle point* for all $K \geq 1$.

B. Analysis of the bifurcation diagram

Using the analysis of the previous subsection, we can see that a bifurcation occurs at $K = 1$. Looking at the bifurcation diagram (Figure 8), we hypothesize that there is a *supercritical pitchfork bifurcation*. In

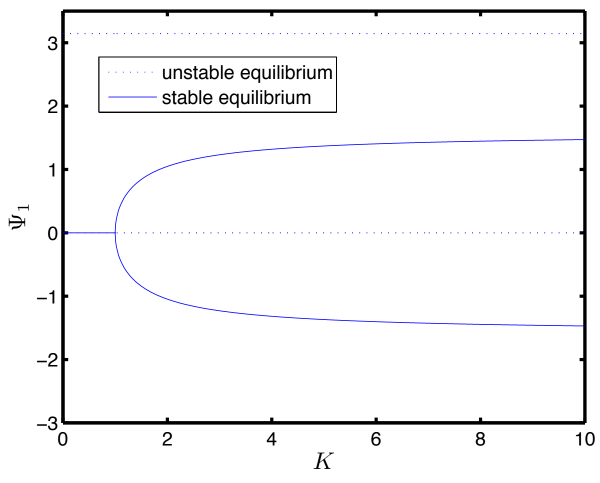

Fig. 8. Bifurcation diagram in the (K, ψ_1) plane, i.e, ψ_1 as a function of bifurcation parameter K fixing $\bar{\theta}_2 = \pi$. At $K = 1$ we have a supercritical pitchfork bifurcation. We have one stable equilibrium for $K < 1$ and for $K > 1$ there are two stable equilibria.

order to prove it, we use the extension for pitchforks of the general theorem for saddle node bifurcations in [13]. There are three conditions to check in the theorem. We define $\boldsymbol{\psi}_0 = (\psi_1, \psi_2)_0 = (0, \pi)$, $K_0 = 1$.

- First condition: nondegeneracy of the linearization $J_0 = \frac{\partial f}{\partial \boldsymbol{\psi}}\Big|_{\boldsymbol{\psi}_0, K_0} = \begin{pmatrix} -\frac{1}{2} & -\frac{1}{2} \\ -\frac{1}{2} & -\frac{1}{2} \end{pmatrix}$, where f is the vector field given by (22) with corresponding state vector $\boldsymbol{\psi} = (\psi_1, \psi_2)$. Hence the linearization of the system at the bifurcation point has a simple zero eigenvalue. We set $v = \begin{pmatrix} 1 \\ -1 \end{pmatrix}$ and $w = \begin{pmatrix} 1 & -1 \end{pmatrix}$ to be respectively the right and left eigenvectors of the linearization for the zero eigenvalue.
- Second condition: transversality condition to control nondegeneracy with respect to the parameter $\frac{\partial^2 f}{\partial \boldsymbol{\psi} \partial K}\Big|_{\boldsymbol{\psi}_0, K_0} = \frac{1}{2} \begin{pmatrix} 1 & -1 \\ -1 & 1 \end{pmatrix}$, this leads to $w.\ \frac{\partial^2 f}{\partial \underline{\psi} \partial K}\Big|_{\underline{\psi}_0, K_0} .v = 2 \neq 0$
- Third condition: transversality condition to control nondegeneracy with respect to the dominant effect of the cubic nonlinear term $w_i v_j v_k v_l\ \frac{\partial^3 f}{\partial \psi_j \partial \psi_k \partial \psi_l}\Big|_{\boldsymbol{\psi}_0, K_0} = -6 < 0$, where i, j, k, l go from 1 to 2.

This last condition completes the proof of the existence of a supercritical pitchfork bifurcation at $(0, \pi)$ for $K = 1$.

Before the bifurcation ($K < 1$), the only stable equilibrium is $\boldsymbol{\psi}_{antisync2} = (0, \pi)$. This corresponds to the case where each informed subgroup follows its own preferred direction; there is no compromise between the individuals and the group splits. When $K < 1$ the strength of the coupling force compared to the preferred direction is too weak to influence the stable steady state of the system. For $K > 1$, there are two stable equilibria, $\boldsymbol{\psi}_{sync1}$ and $\boldsymbol{\psi}_{sync2}$; they correspond, respectively, to the motion in the directions $\Psi = \frac{\bar{\theta}_2}{2} = \frac{\pi}{2}$ and $\Psi = \frac{\bar{\theta}_2}{2} + \pi = \frac{3\pi}{2}$. As we increase the bifurcation parameter K, the two directions ψ_1 and ψ_2 become synchronized. $\bar{\theta}_2 = \pi$ is the only case where we have two stable equilibria for large value of K.

VI. Conclusion

We have studied equilibria, stability and bifurcation for a group of $N = N_1 + N_2 + N_3$ coupled individuals moving in the plane where there are N_1 informed individuals with a preferred direction $\bar{\theta}_1 = 0$, $N_2 = N_1$ informed individuals with a second preferred direction $\bar{\theta}_2$ and $N_3 = 0$ uninformed individuals. We showed that the system has either one or two stable equilibria. The K-almost synchronized motion of the two subgroups in the direction $\Psi = \frac{\bar{\theta}_2}{2}$ is always stable. For some range of the parameters K and $\bar{\theta}_2$ the K-almost synchronized motion of the two subgroups in the direction $\Psi = \frac{\bar{\theta}_2}{2} + \pi$ is stable. In the case $N_1 \neq N_2$, the stable equilibrium does not correspond to $\Psi = \frac{\bar{\theta}_2}{2}$, but rather to a weighted average of 0 and $\bar{\theta}_2$. For example, if $N_1 > N_2$, the stable solution Ψ corresponds to a direction closer to 0 than to $\bar{\theta}_2$. For N_2 fixed and with increasing N_1, the stable equilibrium value of Ψ asymptotically approaches 0 as shown in Figure 9. Likewise for N_1 fixed and with increasing N_2, the stable equilibrium value of Ψ asymptotically approaches $\bar{\theta}_2$.

The reduced model restricted to informed individuals only (i.e., $N_3 = 0$) does not exhibit full synchronization of the group unless the coupling gain K is very large. This means that for the full model (1) the individuals in the population do not fully aggregate and the group splits. In ongoing work, motivated by further simulation studies that reveal factors contributing to aggregation and group decision making, we are developing and studying the dynamics of models that include uninformed individuals and more complicated interconnections.

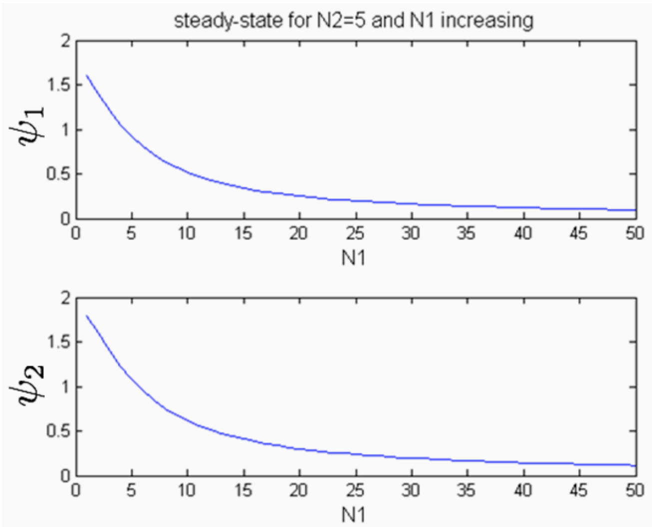

Fig. 9. The equilibrium values of ψ_1 and ψ_2 corresponding to the stable motion $\boldsymbol{\psi}_{sync1}$ as a function of subgroup population size N_1 for fixed subgroup population size $N_2 = 5$. As N_1 increases the stable equilibrium values of both ψ_1 and ψ_2 approach 0, the preferred direction $\bar{\theta}_1$ of the subgroup with dominating population size N_1.

REFERENCES

[1] J. Krause and G. D. Ruxton. *Living in Groups*. Oxford Univ. Press, Oxford, 2002.
[2] I. D. Couzin and J. Krause. Self-organization and collective behaviour in vertebrates. *Advances in the Study of Behavior*, 32:1–75, 2003.
[3] I.D. Couzin, J. Krause, N.R. Franks, and S.A. Levin. Effective leadership and decision making in animal groups on the move. *Nature*, 434:513–516, 2005.
[4] E. Justh and P. S. Krishnaprasad. Equilibria and steering laws for planar formations. *Systems and Control Letters*, 52:1:25–38, 2004.
[5] R. Sepulchre, D. Paley, and N. E. Leonard. Stabilization of planar collective motion: All-to-all communication. *IEEE Transactions on Automatic Control*, 2006. Conditionally accepted.
[6] N. E. Leonard, D. Paley, F. Lekien, R. Sepulchre, D. Fratantoni, and R. Davis. Collective motion, sensor networks and ocean sampling. *Proceedings of the IEEE*, 2006. To appear.
[7] Y. Kuramoto. *Chemical oscillations, waves, and turbulence*. Springer-Verlag, 1984.
[8] R. E. Mirollo and S. H. Strogatz. Jump bifurcation and hysteresis in an infinite-dimensional dynamical system of coupled spins. *SIAM J. Appl. Math.*, 50(1):108–124, 1990.
[9] R. Thom. *Structural Stability and Morphogenesis.* Benjamin, New York, 1972.
[10] T. Poston and I. Stewart. *Catastrophe Theory and its Applications*. Pitman, London, 1978.
[11] M. Lindauer. Communication in swarm-bees searching for a new home. *Nature*, 179:63–67, 1957.
[12] S. Strogatz. *Nonlinear Dynamics and Chaos*. Perseus, 1994.
[13] J. Guckenheimer and P. Holmes. *Nonlinear Oscillations, Dynamical Systems, and Bifurcations of Vector Fields*. Springer-Verlag, New York, 1983.